Photopolymerization of Monolayers Prepared from Surfactants Containing Styrene Moieties

R. Rolandi,[1] R. Paradiso,[1] S. Q. Xu,[2] C. Palmer, and J. H. Fendler*

Contribution from the Department of Chemistry, Syracuse University, Syracuse, New York 13244-1200. *Received October 11, 1988*

Abstract: Monolayers on aqueous surfaces have been prepared from positively and negatively charged synthetic surfactants: bis[2-(*n*-hexadecanoyloxy)ethyl]methyl(*p*-vinylbenzyl)ammonium chloride (**1**), di-*n*-octadecylmethyl(*p*-vinylbenzyl)ammonium chloride (**2**), di-*n*-octadecylmethyl[2-[(4-vinylbenzoyl)oxy]ethyl]ammonium chloride (**3**), *n*-hexadecyl 11-(4-vinylbenzamido)undecyl hydrogen phosphate (**4**), and dioctadecyldimethylammonium bromide (**5**). Surface pressure–surface area, surface potential–surface area, and surface ellipsometry–surface area isotherms have led to values for collapse areas (A_c) and collapse pressures (P_c) of 35 Å^2/molecule and 67 mN/m, 55 Å^2/molecule and 40 mN/m, 70 Å^2/molecule and 42 mN/m, 33 Å^2/molecule and 54 mN/m, and 42 Å^2/molecule and 50 mN/m for monolayers prepared from **1**–**5**, respectively. Ultraviolet irradiation of monolayers prepared from **1**–**4** resulted in their photopolymerization. The A_c value decreased upon polymerization of monolayers prepared from **1** and **2**, but it increased for monolayers prepared from **4**. A similar trend was observed in the surface potential and ellipsometric measurements. Kinetics of photopolymerization of monolayers prepared from **1** have been investigated in detail. Rate constants for the photopolymerization, initiated by steady-state and pulsed-laser irradiations, have been determined at different surface pressures and irradiation energies. The obtained data have been analyzed in terms of a two-dimensional patch-polymerization model (PPM) and by the classical approach considering photoinitiation, propagation, and termination rates (CPM). Both models predict a first-order change of the monolayer surface area as a function of irradiation time. The two models predict, however, different intensity relationships. Plots of the logarithms of photopolymerization rates against the logarithms of light intensities should give a straight line whose slope is 0.5 for the CPM model, but a slope of 1.0 should result for the PPM model. Values of 0.4 and 0.95 have been obtained for the slopes of the plots of the logarithm of polymerization rates vs the logarithm of irradiation intensity for the photopolymerizations mediated by low-intensity steady-state and high-intensity laser irradiations. Apparently, the CPM model is satisfactory at low intensities of irradiation while the PPM model provides a better description of monolayer photopolymerizations mediated by high irradiation energies. Differences between the irradiation intensities also manifest in the average degrees of polymerization ($\bar{L}$ values). $\bar{L}$ values were found to be between 11 and 27 if the monolayer photopolymerization was mediated by high-intensity irradiations. Conversely, at low intensities of irradiation, $\bar{L}$ values as high as 314 were obtained. Photopolymerization of monolayers have been compared to those of vesicles and bilayer lipid membranes.

The theoretical importance and practical utility of two- and three-dimensional molecular organization is increasingly recognized.[3,4] Molecular monolayers and organized multilayers (Langmuir–Blodgett or LB films) have potential applications in active and nonlinear optics; chemical, physical, and biological sensing devices; and surface modification for resists, passivation, and wetting.[5,6] Importantly, they provide matrices for molecular electronic devices.[7] The exponential growth of research activity focused upon monolayers and LB films is hardly surprising.[8]

Development of viable LB films requires long-term mono- and interlayer stabilities and controllable morphologies. Selective polymerization of monolayers provides a means to meet these requirements.[9-18] Indeed, we have shown that polymerization of surfactant vesicles results in their increased stabilities and altered permeabilities and morphologies.[19-24] Advantage has been taken of surfactants which contain styrene in their headgroups [bis[2-(*n*-hexadecanoyloxy)ethyl]methyl(*p*-vinylbenzyl)ammonium chloride (**1**), di-*n*-octadecylmethyl(*p*-vinylbenzyl)ammonium chloride (**2**), di-*n*-octadecylmethyl[2-[(4-vinylbenzoyl)oxy]-ethyl]ammonium chloride (**3**)] or in their tail [*n*-hexadecyl 11-(4-vinylbenzamido)undecyl hydrogen phosphate (**4**)]. Photopolymerizations of vesicles prepared from surfactants **1**–**3** were shown to result in pulling some 10–20 aryl groups together and thereby creating surface clefts.[20,23] Although no morphological information was obtained for polymerized vesicles prepared from **4**, the degree of polymerization was found to be even smaller (2–5) than those in **1**–**3**.[24]

Photopolymerization of monolayers prepared from **1**–**4** is the subject of the present paper. Surface pressure–surface area, surface potential–surface area, and surface ellipsometry–surface area determinations prior and subsequent to polymerizations provided structural information. Kinetics of photopolymerizations,

(1) Present address: Dipartimento di Fisica, Università di Genoa, Italy.
(2) Present address: Department of Modern Chemistry, University of Science and Technology of China, Hefei, China.
(3) Fendler, J. H. *Membrane Mimetic Chemistry*; Wiley-Interscience: New York, 1982.
(4) Fendler, J. H. *Chem. Rev.* **1987**, *87*, 877–899.
(5) Swalen, J. D.; Allara, D. L.; Andrade, J. D.; Chandross, E. A.; Garoff, S.; Israelachvili, J.; McCarthy, T. J.; Murray, R.; Pease, R. F.; Rabolt, J. F.; Wynne, K. J.; Yu, H. *Langmuir* **1987**, *3*, 932–950.
(6) Roberts, G. G. *Adv. Phys.* **1985**, *34*, 475–512.
(7) Carter, F. L. *Molecular Electronic Devices*; Marcel Dekker: New York, 1987.
(8) The number of papers presented at the International Conferences on Langmuir–Blodgett Films increased from 49 in 1982 (see *Thin Solid Films* **1983**, *99*, 1–329), to 79 in 1985 (see *Thin Solid Films* **1985**, *132–134*, 1–736), and to 114 in 1987 (see *Thin Solid Films* **1988**, *159*, 1–478 and *Thin Solid Films* **1988**, *160*, 1–505).
(9) Fendler, J. H. In *Surfactants in Solution*; Mittal, K. L., Lindman, B., Eds.; Plenum Press: New York, 1984; pp 1947–1989.
(10) Dubault, A.; Casagrande, C.; Veyssie, M. *J. Phys. Chem.* **1975**, *79*, 2254–2259.
(11) Letts, S. A.; Fort, T., Jr.; Lando, J. B. *J. Colloid Interface Sci.* **1976**, *56*, 64–75.
(12) Day, D. R.; Ringsdorf, H. *Makromol. Chem.* **1979**, *180*, 1059–1063.
(13) O'Brien, K. C.; Rogers, C. E.; Lando, J. B. *Thin Solid Films* **1983**, *102*, 131–140.
(14) Hupfer, B.; Ringsdorf, H. *Chem. Phys. Lipids* **1983**, *33*, 263–282.
(15) Holden, D. A.; Ringsdorf, H.; Haubs, M. *J. Am. Chem. Soc.* **1984**, *106*, 4531–4536.
(16) Elbert, R.; Laschewsky, A.; Ringsdorf, H. *J. Am. Chem. Soc.* **1985**, *107*, 4134–4141.
(17) Higashi, N.; Kunitake, T. *Chem. Lett.* (*Jpn*) **1986**, 105–108.
(18) Laschewsky, A.; Ringsdorf, H.; Schmidt, G.; Schneider, J. *J. Am. Chem. Soc.* **1987**, *109*, 788–796.
(19) Fendler, J. H.; Tundo, P. *Acc. Chem. Res.* **1984**, *17*, 3–7.
(20) Reed, W.; Guterman, L.; Tundo, P.; Fendler, J. H. *J. Am. Chem. Soc.* **1984**, *106*, 1897–1907.
(21) Nome, F.; Reed, W.; Politi, M.; Tundo, P.; Fendler, J. H. *J. Am. Chem. Soc.* **1984**, *106*, 8086–8093.
(22) Serrano, J.; Mucino, S.; Millan, S.; Reynoso, R.; Fucugauchi, L. A.; Reed, W.; Nome, F.; Tundo, P.; Fendler, J. H. *Macromolecules* **1985**, *18*, 1999–2005.
(23) Reed, W.; Lasic, D.; Hauser, H.; Fendler, J. H. *Macromolecules* **1985**, *18*, 2005–2012.
(24) Yuan, Y.; Tundo, P.; Fendler, J. H. *Macromolecules* **1988**, in press.

0002-7863/89/1511-5233$01.50/0

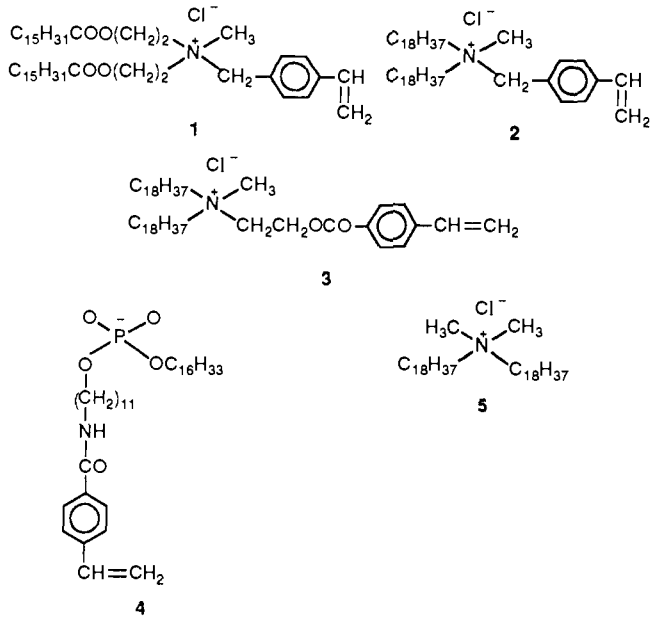

followed by monitoring surface-area changes, were interpreted in terms of previously developed models. Good agreement was obtained between experiments carried out at the Dipartimento di Fisica della Università di Genoa, at the Centre de Recherche en Photobiophysique of the Université du Québec à Trois-Rivières, and at the Chemistry Department of Syracuse University.

Experimental Section

Materials. Preparation, purification, and characterization of the surfactants **1**–**4** and dioctadecyldimethylammonium bromide (**5**) have been described.[20-24] Spectroscopic-grade chloroform, the spreading solvent, was used as received. Reagent-grade NaCl was baked at 800 °C for several hours (in Genoa and Syracuse) or extracted with $CHCl_3$ and baked (at Trois-Rivières). Water was purified in Syracuse by using a Millipore Milli-Q filter system provided with a 0.22 μm Millistack filter at the outlet. In Genoa, the water was bidistilled in a homemade quartz distillation unit. In Trois-Rivières, the water used was triply distilled with a Heraus-based quartz unit. Specific resistivity was, typically, 18 MΩ cm at 25.0 °C with a measured surface tension of ≥71 mN m^{-1}, as determined by the DuNouy method. Nitrogen was high-purity dry grade (Union Carbide).

Monolayer Formation. The same protocol was followed for monolayer formation at the three different locations. Spreading solutions were prepared by dissolving the monomeric surfactants in spectroscopic-grade chloroform at concentrations of 1–8 mg/mL. Nitrogen atmosphere in the trough was maintained during spreading, solvent evaporation, and measurements. The surface of the aqueous solution, contained in the trough, was cleaned several times prior to monolayer formation by sweeping with a Teflon barrier. The subphase was deemed clean when the surface-pressure increase was less than 0.2 dyn/cm upon compression to $^1/_{20}$ of the original area and when this surface pressure increase remained the same subsequent to aging for several hours (criteria of minimal aging of the surface).[25] An appropriate amount of the spreading solutions (10–100 μL) was carefully injected onto the cleaned, thermostated, aqueous surface. Measurements commenced 5–30 min subsequent to monolayer formation. Differences between the concentration, the amount, and the rate of compression of the spreading solution are believed to be responsible for the minor differences in the isotherms determined in Genoa, Trois-Rivières, and Syracuse (vide infra).

Monolayer Characterizations. Monolayers were characterized by surface pressure vs surface area, surface potential vs surface area, and ellipsometry vs surface area determinations.

A commercial Lauda Model P Langmuir Film Balance was used in Syracuse for obtaining surface pressure–surface area isotherms. The compression rate was ca. (2–5) × 10^{-3} Å^2 per molecule per s. The film balance was vibrationally isolated by placing it on a Micro-g optical table. The entire assembly of the optical table and film balance was enclosed in a Class 100 (HEPA filter) hood. Facilities were provided for nitrogen inlet and illumination. The output of the film balance was coupled to a Zenith microcomputer and a Hewlett-Packard x-y recorder.

(25) Mingins, J.; Owens, N. F. *Thin Solid Films* **1987**, *152*, 9–28.

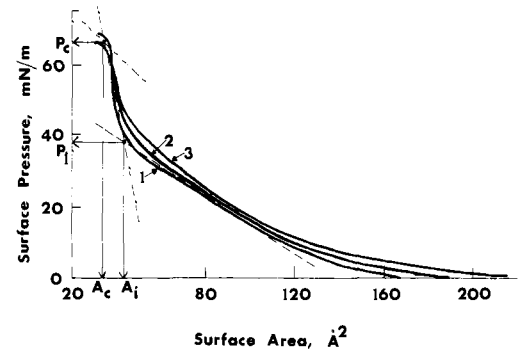

Figure 1. Surface area–surface pressure isotherms for spreading **1** on aqueous 5.0 mM NaCl in Genoa (1), Syracuse (2), and Trois Rivières (3). Areas (A_i) and pressures (P_i) associated with the transition to a compressed state were taken by projecting the intersection of straight lines drawn to the appropriate sections of the isotherm to the surface area and surface pressure axes. Collapse areas (A_c) and collapse pressures were taken by treating that transition similarly.

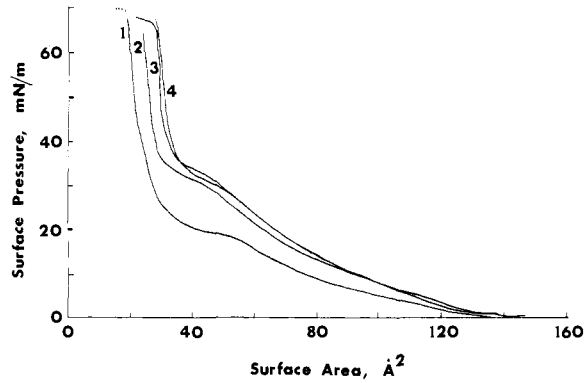

Figure 2. Surface pressure–surface area isotherms for spreading **1** on water (1) and on 1.7 (2), 5.0 (3), and 50 mM (4) NaCl.

A circular, temperature-controlled film balance, equipped with a Wilhelmy plate (type RCM-2 Mayer-Feintecknik, Göttingen), was used in Genoa. The film balance was enclosed in a Faraday cage. Surface pressure–surface area isotherms were taken at 0.1–0.8 Å^2 per molecule per second compression. During compression, the film area typically changed from 340 to 40 cm^2. Surface potentials were measured by a 610 BR Keithley Electrometer, connected to an ^{241}Am air-ionizing electrode, suspended at ca. 5 mm above the monolayer. Ground connection was provided by a Ag/AgCl electrode.

Several home-constructed Langmuir film balances were used at Trois-Rivières for obtaining surface pressure–surface area and surface potential–surface area measurements,[26] at compression rates of ca. (2–5) × 10^{-3} Å^2 per molecule per second. Some of the film balances were in a Class 10 clean room. Construction and calibration of the ellipsometer used for measurements of monolayers at water–air (or N_2) surfaces have been described previously.[27]

Monolayer Polymerizations. Monolayers, formed from surfactants **1**–**4**, were polymerized by irradiation with ultraviolet light in a nitrogen atmosphere at all three sites. In Syracuse and Trois-Rivières, a 4-W UV lamp was placed 2 cm above the surface of the monolayer. The light intensity was determined to be 10 ± 2 μW/cm^2 at 250 ± 3 nm by a Model 2232 UV optical power meter (Mimir Instruments Corp.).[28] In Genoa, a 200-W mercury lamp was used to illuminate a 40-cm^2 surface via a parabolic mirror. The light intensity was determined to be 10 ± 3 mW/cm^2 between 220 and 300 nm (the intensity between 220 and 270 nm was very low, approximately 0.2 μW/cm^2).

Monolayers, prepared from **1**, were also polymerized, in Syracuse, by irradiation by repetitive laser pulses. The fourth harmonic of a Quanta-Ray DCR 1A Nd:YAG laser was used to provide 15-ns, 8.9-mJ pulses

(26) Munger, G.; Lorrain, L.; Gagné, G.; Leblanc, R. M. *Rev. Sci. Instrum.* **1987**, *58*, 285–288. Dijkmans, H.; Munger, G.; Aghion, J.; Leblanc, R. M. *Can. J. Biochem.* **1981**, *59*, 328–331.

(27) Ducharme, D.; Tessier, A.; Leblanc, R. M. *Rev. Sci. Instrum.* **1987**, *58*, 571–578.

(28) We are grateful to the semiconductor electronics group of General Electric Corp., Syracuse, New York, for permitting us to use their power meter.

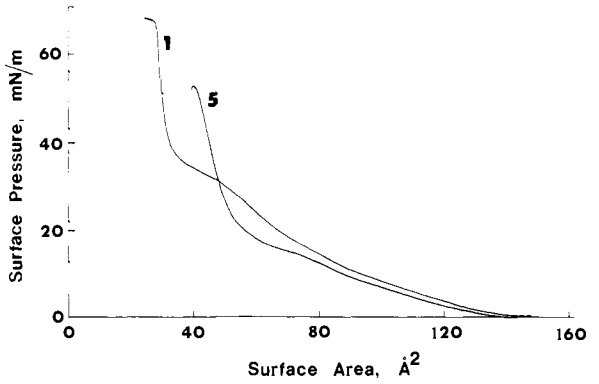

Figure 3. Surface pressure–surface area isotherms for spreading **1** and **5** on 5.0 mM NaCl.

at a rate of 10 Hz. The laser beam was focused onto the monolayer surface and expanded to an area of 110 cm^2 by appropriate lenses and mirrors. Laser intensities were measured by a Scientech 362 power meter.

Results

Isotherms for Nonpolymerized Monolayers. The surface pressure–surface area isotherm for **1**, spread on 5.0 mM aqueous NaCl in three different troughs at three different times in three different locations, is shown in Figure 1. Considering that different samples of **1** were prepared with chloroforms of different origin and that they were spread in different manners, the agreement between the results obtained in Genoa, Trois-Rivières, and Syracuse is quite satisfactory. At low surface pressure, as expected, molecules lie on the water surface, occupying large areas. With increasing surface pressure, they begin to associate and orient their hydrophobic tails away from the surface. Following a partially and more fully condensed state, there is a transition to a compressed (solid) state at a transition pressure, P_t = 38 mN/m. The average area per one molecule occupied in this state, A_i, was found to be 46 $Å^2$ by extrapolating the straight-line portion of the solid-state isotherm to zero pressure. The method of taking A_t, A_c, P_c, and P_i values for surface pressure–surface area isotherms is illustrated in Figure 1. The equation of state of the solid monolayer is characterized by a relatively small change in the area with increasing surface pressure. This state prevails until the collapse of the monolayer, characterized by the collapse pressure, P_c (67 mN/m, Figure 1).

The presence of electrolytes in the subphase was found to profoundly influence the spreading behavior of **1**. As seen in Figure 2, addition of 1.7 and 5.0 mM NaCl resulted in increased P_t and A_c values. Addition of further amounts of NaCl led to saturation behavior. Similar effects were observed in the surface potential–surface area measurements.

It is instructive to compare the isotherms of **1** and **5**. Compound **5** does not contain the styrene moiety. From the isotherms determined for **1** and **5** (Figure 3), values of 35 and 42 $Å^2$/molecule have been obtained for A_c (Table I). Projections of CPK space-filling models (Ealing Corporation) lead to a headgroup area of 31 $Å^2$/molecule for **1**.

In Figure 4, typical surface pressure vs surface area, surface potential vs surface area, and ellipsometry vs surface area isotherms for **1** on 5.0 mM NaCl are shown. Similar plots for **4** under identical conditions are collected in Figure 5. Means of A_i, A_c, P_c, and P_i values determined for monolayers prepared from different surfactants at the three different locations are gathered in Table I.

Isotherms for Polymerized Monolayers. Irradiation of monolayers formed from **1**, **2**, **3**, and **4** by ultraviolet light resulted in pronounced changes of their isotherms. After the completion of irradiation (typically 30 min), the monolayers were allowed to expand and they were then recompressed to determine the isotherm for the polymerized monolayer. Completion of the polymerization was confirmed by taking infrared spectra of a monolayer deposited on calcium fluoride plates prior and subsequent to exposure to ultraviolet radiation.[29] Surface pressure vs surface area, surface potential vs surface area, and ellipsometry vs surface area of nonpolymerized and polymerized (at 40 mN/m pressure) monolayers prepared from **1** and **4**, respectively, are compared in

Table I. Surface Pressure–Surface Area Isotherms[a]

compound	A_i, $Å^2$	A_c, $Å^2$	P_c, mN/n	P_i, mN/n
nonpolymerized **1**	46	35	67	38
polymerized **1**	54	32	53	
nonpolymerized **2**	110	55	40	
polymerized **2**	86	54	25	
nonpolymerized **3**	120	70	42	
polymerized **3**	120	70	42	
nonpolymerized **4**	46	33	54	25
polymerized **4**	58	48	29	
5	58	42	50	

[a] See the Experimental Section for description of spreading conditions. Values are the means of 18 determinations for nonpolymerized and polymerized **1** (error ±6%), 2 determinations for nonpolymerized and polymerized **3** (error ±25%), 10 determinations for nonpolymerized and polymerized **4** (error ±8%), and 4 determinations of **5** (error ±15%). At 25.0 °C, unless stated otherwise. Subphase 5.0 mM NaCl. Compression speed = (1–5) × 10^{-3} $Å^2$/molecule per second. See Figure 1 for definition of A_i, A_c, P_c, and P_i.

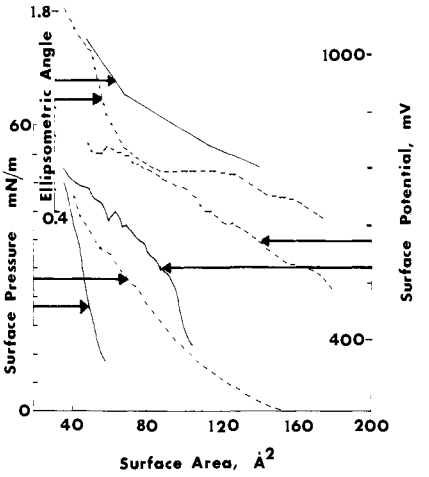

Figure 4. Surface pressure–surface area, surface potential–surface area, and ellipsometric angle–surface area isotherms for spreading monolayers prepared from **1** on 5.0 mM NaCl prior (– –) and subsequent (—) to photopolymerization. Polymerization was carried out at 40 mN/m.

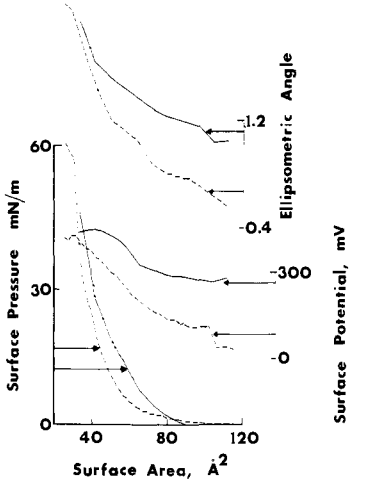

Figure 5. Surface pressure–surface area, surface potential–surface area, and ellipsometric angle–surface area isotherms for spreading monolayers prepared from **4** on 5.0 mM NaCl prior (– –) and subsequent (—) to photopolymerization. Polymerization was carried out at 40 mN/m.

(29) Palmer, C. Unpublished work, 1988.

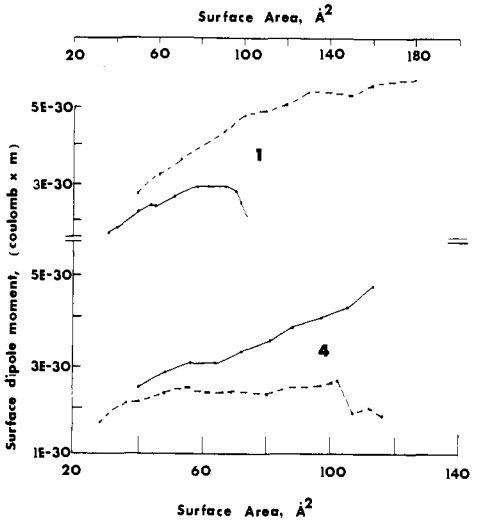

Figure 6. Surface dipole moments vs surface area isotherms using eq 1 for monolayers prepared from **1** and **4** prior (--) and subsequent (—) to photopolymerization. Polymerization was carried out at 40 mN/m.

Figures 4 and 5. Isotherms of these two surfactants undergo completely different changes upon irradiation by ultraviolet light. Irradiation of the monolayers prepared from **1** resulted in an appreciable decrease of the area occupied per molecule and in the collapse pressure. The trend is similar for the isotherms obtained by surface potential and ellipsometry. The voltage change (V), determined in the monolayer surface potential measurements, is related to the apparent dipole moment at the gas–liquid interface, μ, by

$$\mu = \epsilon_0 \epsilon a (V - \psi_0) \tag{1}$$

where ϵ_0 is the permittivity constant of the free space, ϵ is the mean dielectric constant at the gas–liquid interface, a is the area occupied by a surfactant molecule, and ψ_0 is the potential due to the electric double layer at the surfactant–aqueous solution interface. The value of ψ_0 was obtained from the Gouy–Chapman equation:

$$\sinh \frac{\psi_0 e}{2\mathbf{k}T} = \frac{\sigma}{(8NC\epsilon_0\epsilon_w \mathbf{k}T)^{1/2}} \tag{2}$$

where e is the electronic charge, $\mathbf{k}$ is Boltzmann's constant, N is Avogadro's number, T is the absolute temperature, σ is the surface charge density, C is the electrolyte concentration in the subphase (5×10^{-3} M), and ϵ_w is the dielectric constant of water. In eq 1 and 2, ϵ is the mean of the dielectric constants characterizing three different regions: the hydrocarbon chains of the surfactant, the headgroup of the surfactant, and the oriented water molecules surrounding the polar headgroups of the surfactants. Uncertainties in knowing the boundaries of the different regions and values of their respective dielectric constants necessitated taking $\epsilon = 1$. σ has been evaluated by assuming that each surfactant molecule carries a positive charge and that contribution of counterions can be neglected. In Figure 6, the apparent surface dipole moments of monolayers prepared from **1** and **4** prior and subsequent to polymerizations are compared. Decreases in μ upon polymerization can be taken to imply molecular reorientations assuming that ϵ remains unchanged. The change of surface potential upon polymerization can also be due to the change of the counterion absorption and hence to the change of surface charge density (σ in eq 2).

For UV polymerization of **1**, the presence of a plateau in the ellipsometric angle vs surface area isotherm suggests the absence of molecular reorganization between 70 and 130 Å²/molecule (Figure 4).[30] This is based on the assumption that the trend of increasing ellipsometric angle with decreasing surface area occupied per molecule is due (i) to an increase in the monolayer thickness in the liquid expanded state and (ii) to an increase of the index of refraction in the liquid condensed state. The simultaneous presence of large fluctuations in the surface potential is an indication of the formation of clusters of oriented molecules.

(30) The "ellipsometric angle" is the phase shift $\delta\Delta = \Delta - \bar{\Delta}$ where Δ is the clean surface phase change measured on film surface and $\bar{\Delta}$ is the phase change on the clean surface.[27]

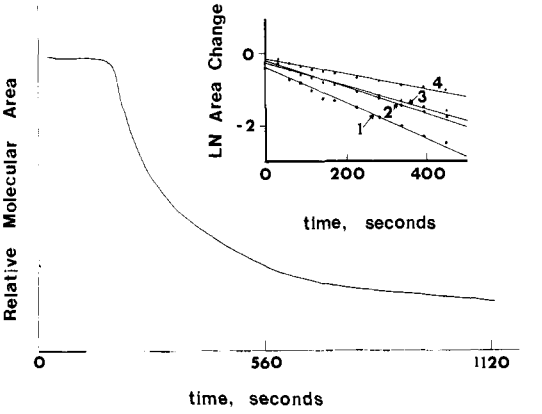

Figure 7. A typical change of the surface area of a monolayer prepared from **1** at a constant pressure as a function of steady-state-irradiation time. The insert shows logarithmic plots used to calculate the decay times (τ values in eq 25, Appendix) for monolayers kept at 36 (1), 26 (2), and 21 mN m^{-1} (3) and $\bar{\epsilon}\bar{I} = 3.0 \times 10^{-4}$; and at 26 mN m^{-1} and $\bar{\epsilon}\bar{I} = 1.0 \times 10^{-4}$ (4).

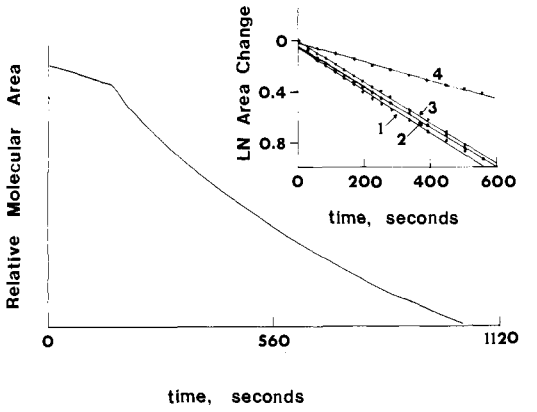

Figure 8. A typical change of surface area of a monolayer prepared from **1** at a constant pressure as a function of irradiation by repetitive laser pulses. The insert shows the logarithmic plots used to calculate the decay times for monolayers kept at 25 mN m^{-1} at 0.8 (1), 1.9 (2), 2.8 (3), and 3.6 mW/pulse (4) energies.

Irradiation of monolayers prepared from **4** did not decrease the area occupied per molecule at a fixed surface pressure of 400 mN/m. Surface potential and ellipsometry changes paralleled this behavior (Figure 5). Values of A_l, A_c, and P_c for photopolymerized monolayers prepared from **1**–**4** are included in Table I.

Kinetics of Monolayer Photopolymerization. Kinetics of photopolymerization of monolayers prepared from **1** could be followed, at different surface pressures and at different light (or laser) intensities, by monitoring the changes of surface areas as a function of irradiation time. In Figure 7, a typical plot is shown for this change upon steady-state irradiation. The logarithmic plots of surface area changes vs steady-state-irradiation times are seen (in the insert of Figure 7) to be described by a pseudo-first-order process. The lifetimes of these processes depend on the surface pressure and light intensity.

Irradiation by repetitive laser pulses caused similar decreases in the surface areas of the monolayers of **1**, kept at a given pressure. Figure 8 shows such a typical behavior. The insert in Figure 8 illustrates logarithmic plots of these area changes as a function of the time the monolayer has been exposed to repetitive laser pulses. It should be pointed out that prior to the completion of the polymerization, initiated either by a steady-state lamp or by a pulsed laser, stopping the irradiation interrupts the surface

Table II. Kinetics of Photopolymerization of Monolayers Prepared from **1**[a]

surface pressure, mN m^{-1}	irradiation intensity[b]	τ, s[c]	$\bar{L}$[d]	τ_{av}, s[e]	k_p/k_t[e]
		Steady-State Irradiations			
5[f]	2.0×10^{-5}	2220	214		
15[f]	2.0×10^{-5}	1875	252		
35[f]	2.0×10^{-5}	1500	314		
35[f,g]	2.0×10^{-5}	2220	214		
11[h]	3.0×10^{-4}	163 (0.990)	193	89	2.9
21[h]	3.0×10^{-4}	205 (0.997)	153	244	7.6
36[h]	3.0×10^{-4}	94 (0.981)	335	182	12.2
45[h]	3.0×10^{-4}	135 (0.991)	223	397	14.5
26[h]	3.0×10^{-4}	145 (0.982)	217		
26[h]	1.1×10^{-4}	333 (0.914)	258		
26[h]	2.7×10^{-5}	556 (0.975)	628		
26[h]	9.9×10^{-6}	595 (0.993)	1602		
		Laser-Initiated Polymerizations			
25[h]	0.8	3070		127	0.24
25[h]	1.9	897	11	1.3	0.0024
25[h]	2.8	1053	17	2.9	0.17
25[h]	3.6	980	13	33	0.18

[a] Ambient temperature, 5.0×10^{-3} M NaCl as subphase. [b] Expressed as $\bar{\epsilon}\bar{I}$ for steady-state irradiations and mW/pulse for laser-pulse-initiated photolysis. See ref 37 for details. [c] Correlation coefficients are in parentheses. [d] Deterimined by means of eq 6. [e] Determined by means of eq 8. [f] Experiments carried out in Genoa. [g] Determined in monolayers prepared from **2**. [h] Experiments performed in Syracuse.

area change. Upon the restart of irradiation, the area of the monolayer continues to decrease at the same rate as it did before. In general, faster rates of photopolymerizations were observed at higher surface pressures. Apparent lifetimes for the photopolymerization of monolayers, calculated from plots similar to those shown in the inserts of Figures 7 and 8, are collected in Table II.

Discussion

Effects of Polymerization on Two-Dimensional Molecular Organization. An important advantage of monolayers is that two-dimensional molecular organization and reactivity can be studied under controlled conditions.[31,32] The surfactants utilized here differ from the usual phospholipids in two respects. First, they contain a quaternary ammonium (**1–3** and **5**) or phosphonate (**4**) headgroup and, thus, they are highly charged and have high surface charge densities. In contrast, the most frequently investigated lipid, lecithin, is zwitterionic. Second, these surfactants have bulky polymerizable styrene moieties on their headgroups (**1–3**) or in their hydrocarbon tail (**4**). These structural factors are expected to influence the spreading behavior of the synthetic surfactants used here and their two-dimensional polymerizations. When **1** is spread on pure water it forms unstable films, the pressure–area isotherms show poor reproducibility, and the collapse, which is not well-defined, occurs at very small values of area/molecule (~10 Å^2/molecule). For **1**, the observed increases in A_i and P_i values on spreading the surfactants on aqueous NaCl instead of on pure water (Figure 2) can be the consequence of decreased solubility in the subphase. This, in turn, is likely to be related to the altered surface charge densities surrounding the surfactant headgroups at the water–air interface. Similar effects of electrolytes, dissolved in the subphase, have been observed on the phase-transition behavior of phosphatidic acid monolayers. The fluid to gel transition pressure (P_i) and the area occupied by L-α-dimyristoylphosphatidic and L-α-dilaurylphosphatidic acids in monolayers were found to increase with increasing monovalent ion concentration dissolved in the subphase.[33] The salinity of the subphase seems to be less crucial for **4**, which forms stable films in both water and salt solution. In 5 mM NaCl, the force–area curves are more expanded and the surface potential is higher (Figure 5).

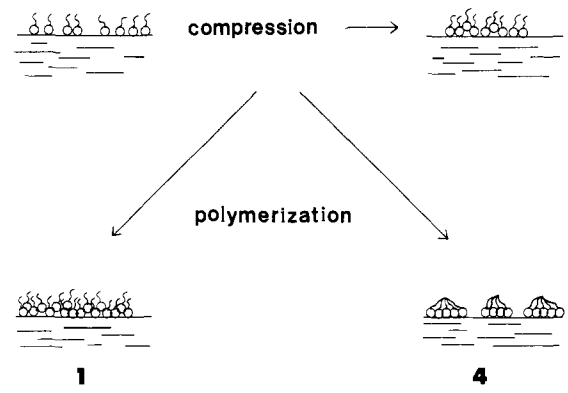

Figure 9. An artist's conception of the compression and polymerization of monolayers prepared from **1** and **4**.

The surface pressure–surface area isotherm of monolayers prepared from nonfunctionalized surfactant **5** indicated a phase transition between 60 and 95 Å^2 per molecule and a limiting area of 40–43 Å^2 per molecule at a surface pressure of 50 mN/m (Figure 3). This experimentally observed limiting surface area corresponds well to that occupied by dialkyldimethylammonium halide surfactants (~40 Å^2/molecule).[34]

The styrene moiety, present in the headgroups of **1–3**, is sufficiently hydrophobic to be directed away from the aqueous subphase. Most likely, it is aligned along the hydrocarbon tails of the surfactants. Thus, the surface area occupied by a molecule of **1** (or that of **2** or **3**) is expected to be larger than that taken up by **5**. Contrary to this expectation, the collapse area of monolayers prepared from **1** (35 Å^2, Table I) is somewhat smaller than those made from **5** (42 Å^2, Table I). However, this modest decrease in the limiting surface area is accompanied by a marked increase of the collapse pressure for monolayers prepared from **1** (67 mN/m, Table I) as compared to those obtained from **5** (50 mN/m, Table I). These results can be rationalized by assuming puckered packing of the monolayers prepared from **1** at high surface pressure. In puckered monolayers, as seen in Figure 9, the surfactants are more tightly packed and, therefore, on the average occupy smaller areas than their nonpuckered counterparts. Puckering becomes more difficult, if not impossible, on spreading the monolayers much below the fluid-to-solid phase transition of the surfactant. Indeed, the surface pressure–surface area isotherms of monolayers prepared from **1** at 10 °C were found to be less condensed at low pressure, more expanded at pressures greater than 45 mN/m, and collapsed at about 53 mN/m. Apparently, at lower temperatures, the less fluid surfactants become less amenable to puckering.

The polymeric film was found to undergo relaxation. For example, steady-state irradiation of a monolayer, prepared from **1** at π = 35 mN/m, decreased the surface area from 45 to 33 Å^2/molecules. The polymerized film was then allowed to expand to a surface area of 100 Å^2/molecules (π = 0). On recompression to π = 35 mN/m, the surface area increased to 37 Å^2/molecule. Polymerized monolayers prepared from diacrylic ester were shown to undergo similar relaxation upon expansion and recompression.[10]

Polymerization of monolayers, prepared from **1**, results in decreased average areas occupied by the surfactants as a consequence of pulling the surfactant headgroups together at the water–air interface (see Figure 9). Polymerization of diacetylene monolayers has also resulted in decreased areas occupied per molecule.[12-16] At high pressures, the puckered structures are likely to be maintained. At lower pressure, liquid-condensed polymerized films are formed.

Polymerization of the styrene moiety in **4** ties some of the surfactant tails together. This translates into a somewhat increased

(31) Gaines, G. L., Jr. *Insoluble Monolayers at Liquid–Gas Interfaces*; Interscience: New York, 1966.
(32) Gershfeld, N. L. *Ann. Rev. Phys. Chem.* **1976**, *27*, 349–368.
(33) Lösche, M.; Helm, C.; Mattes, H. D.; Möhwald, H. *Thin Solid Films* **1985**, *133*, 51–64.
(34) Israelachvili, J. N. *Intermolecular and Surface Forces with Applications to Colloidal and Biological Systems*; Academic Press: London, 1985.

effective area which the headgroups occupy. A similar situation has been encountered in the polymerization of octadecylfumarate[35] and in the polycondensation of amino acids on monolayers. Polypeptides formed from $CH_3(CH_2)_{15}CH(NH_2)COO(CH_2)_{21}CH_3$ and $CH_3(CH_2)_{23}CH(NH_2)COO(CH_2)_{21}CH_3$ were found to occupy greater areas at air–water interfaces than their parent amino acids.[36]

Mechanism of Monolayer Photopolymerization. Photopolymerization of monolayers, prepared from **1**, at constant surface pressure results in the monotonic decrease of the surface area as a function of the irradiation time. The rate of decrease depends, as seen in Figure 7, on surface pressure. Assuming that every double-bonded monomer occupies an area a_M larger than the area a_m occupied by the saturated monomer, the area of the monomer at irradiation time t is given by

$$A(t) = a_M M(t) + a_m m(t) \tag{3}$$

where $M(t)$ is the number of double-bonded monomers and $m(t)$ is the number of saturated monomers. Calling $A_o = a_M M_o$, where M_o is the double-bonded monomer number at $t = 0$ and recognizing that the polymerization does not change the overall number of monomers, one obtains

$$\frac{A(t) - A_o}{A_o} = \left(\frac{a_M - a_m}{a_M}\right)\left(\frac{M(t) - M_o}{M_o}\right) \tag{4}$$

Equation 4 relates the area variation with the variation of the monomer number as a function of irradiation time.

The obtained data have been analyzed in terms of a two-dimensional patch-polymerization model (PPM)[20] and by the classical approach considering photoinitiation, propagation, and termination rates (CPM).[37] Full derivation of these two treatments are provided in the Appendix in the Supplementary Material. The PPM model leads to eq 5 and 6 for steady-state irradiations, where τ is the decay time of photopolymerization,

$$\frac{A(t) - A_o}{A_o} + \frac{a_M - a_m}{a_M} = \frac{a_M - a_m}{a_M} e^{-t/\tau} \tag{5}$$

$$\bar{L} \simeq \frac{k_p}{k_m} \simeq \frac{1}{\Phi_r \bar{I} \bar{\epsilon} \tau} \tag{6}$$

Φ_r is the quantum efficiency for radical formation, $\bar{I}$ is the mean intensity of the light source, $\bar{\epsilon}$ is the absorption cross section of the monomer,[38] and $\bar{L}$ is the average length of polymer chains.

Plots of the logarithms of the left-hand side of eq 5 against irradiation times should yield straight lines from which the decay times, τ values, could be obtained. Experimental data, obtained for the photopolymerizations of monolayers prepared from **1**, could be best accommodated in terms of a pseudo-first order process on treatment according to eq 5 (see inserts of Figures 7 and 8).

The $\bar{L}$ values, assessed from eq 6 with the obtained kinetic data, are also given in Table II.

Treating the laser-pulse-initiated-polymerization data in terms of the PPM model results in:

$$\bar{L} \simeq \frac{k_p}{k_m} \simeq \frac{\eta}{\Phi_r \bar{\epsilon} \bar{E}} \tag{7}$$

where η is defined as the fraction of the double-bonded monomers consumed after the completion of the photochemical events initiated by a single laser pulse.

The $\bar{L}$ values obtained from laser-initiated photopolymerizations (eq 36, Appendix) are also included in Table II.

The CPM model leads to eq 8:

$$\frac{\Delta[n]}{[n]} = \frac{k_p}{k_t} \frac{1}{\tau_{av}} t - \frac{k_p}{k_t} \ln 2 \tag{8}$$

which allows the calculation of the average radical chain lifetime, τ_{av}, from the change of monomer concentration, $\Delta[n]$. Typical plots of the data according to eq 50 (Appendix) are given in Figure 10 and τ_{av} and k_p/k_t values are collected in Table II.

Both the PPM and the CPM models predict a first-order change of the monomer surface area as a function of the irradiation time. The two models predict, however, different intensity relationships.

The PPM model is governed by eq 9:

$$R_{PPM} = \frac{1}{\tau} = \Phi_r \bar{\epsilon} \bar{I} \frac{k_p}{k_m + k_s} \tag{9}$$

Thus a plot of the logarithm of the photopolymerization rate

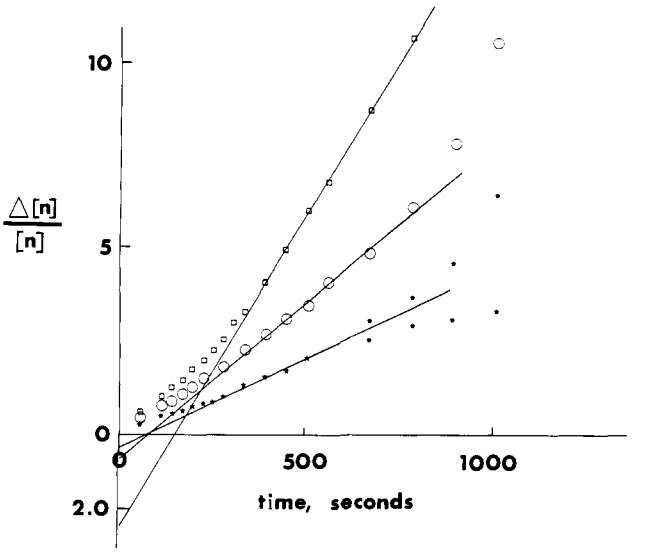

Figure 10. Plots of $\Delta[n]/[n]$ against time (eq 50, Appendix) for the photopolymerization of monolayers prepared from **1** at 11 (□), 21 (○) and 36 (★) mN m^{-1}.

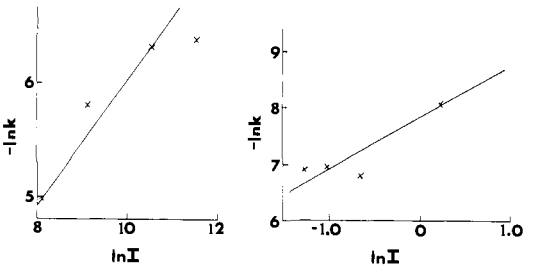

Figure 11. Plots of the logarithm of polymerization rates against the logarithm of intensities of steady-state (left-hand side) and laser (right-hand side) irradiations of monolayers prepared from **1**.

(35) Rabe, J. B.; Rabolt, J. F.; Brown, C. A.; Swalen, J. D. *J. Chem. Phys.* **1986**, *84*, 4096–4102.

(36) Folda, T.; Gros, L.; Ringsdorf, H. *Makromol. Chem., Rapid Commun.* **1982**, *3*, 167–176.

(37) Flory, P. J. *Principles of Polymer Chemistry*; Cornell University Press: Ithaca, NY, 1953; p 111.

(38) The value of Φ_r has been determined to be 0.106.[20] The molar extinction coefficient (ϵ_{266} nm = 1600 M^{-1} cm^{-1}) was converted to a molecular cross section by

$$\epsilon_{266}\text{ nm} = 1.6 \times 10^3\ \text{M}^{-1}\ \text{cm}^{-1}\ L \frac{10^3\ \text{cm}^3}{L} \times \frac{1\ \text{mol}}{6.02 \times 10^{23}\ \text{monomer}} = 2.7 \times 10^{-18}\ \text{cm}^2/\text{monomer}$$

Table II gives $\bar{\epsilon}\bar{I}$ = Integral ($\lambda_1 \rightarrow \lambda_2$) of $\bar{\epsilon}\bar{I}d\lambda$) values for steady-state-irradiation intensities. In Genoa, due to the low reflectivity of the parabolic mirror, the light intensity was almost 0 up to 260 nm and it increased very fast from 280 to 320 nm. Under this condition, the value of absorbed light (i.e., the integral in dλ) rapidly changed with the upper integration limit, λ_2. For example, there was a factor of 26 between λ_2 = 300 nm and λ_1 = 290 nm. This introduced large systematic errors into the calculations of $\bar{L}$. In Syracuse, this error was minimized by the use of a very narrow band path ($^1/_2$ HBW = 5 nm) and by carrying out the integration between 243 and 250 nm for determining $\bar{\epsilon}\bar{I}$ values. The $\bar{L}$ values determined in Syracuse are considered to be more reliable. Nevertheless, the agreement between the $\bar{L}$ values obtained in Genoa at $\bar{\epsilon}\bar{I} = 2.0 \times 10^{-5}$ and π = 35 mN m^{-1} (L = 314) and that in Syracuse at $\bar{\epsilon}\bar{I} = 9.6 \times 10^{-6}$ and π = 26 mN m^{-1} (L = 170) is quite satisfactory. For the laser-initiated photolysis, $\bar{E}$ values are given in Table II as mW/pulse. They were converted to photons/cm^2 for use in eq 37 (Appendix) by dividing by $h\nu$.

(R_{PPM}) against irradiation intensity, $\bar{I}$, should give a straight line with a slope of 1.0. Conversely, the CPM model is given by eq 10:

$$V_R = V_p = k_p[M]\left(\frac{k_o}{k_t}\right)^{1/2}\bar{I}^{1/2} \qquad (10)$$

which indicates that a plot of the logarithm of the photopolymerization rate (V_R) against $\bar{I}$ should give a straight line with a slope of 0.5.

Figure 11 shows such plots for the photopolymerization of monolayers formed from **1**. The slopes obtained in the steady-state and laser-initiated photopolymerization were found to be 0.4 and 0.95, respectively. Apparently, the two-dimensional patch model satisfactorily describes photopolymerizations at high irradiation intensities. Conversely, at lower levels of irradiation, the classical treatment is a better description of the photopolymerization of monolayers prepared from **1**. Interestingly, sufficient data has been reported for the irradiation intensity dependency of diacrylic ester photopolymerization.[10] We have plotted the published data in the forms of log k vs log I and obtained a straight line with a slope of 0.8.

Comparison of Photopolymerizations of 1 in Monolayers, Bilayers, and Vesicles. The work reported here allows a fruitful comparison of the photopolymerization of **1** in monolayers, bilayer lipid membranes (BLMs),[38] and vesicles.[20] Uncertainties in the absolute value of $\bar{L}$ are, of course, recognized. Since the same assumptions were used in treating photopolymerizations of **1** in the different mimetic systems under different conditions, profitable comparisons of the relative magnitude of $\bar{L}$ values can be made between monolayers and vesicles and between irradiations of monolayers at different surface pressures.

Appreciable degrees of monolayer photopolymerization is the most significant observation of the present work. At low-intensity irradiations (Genoa experiments), the average chain length ($\bar{L}$) of polymers are found to increase from 214 to 314 on increasing the surface pressure from 5 to 35 mN/m during the steady-state irradiation of **1** (Table II). This is the expected consequence of tighter packed, puckered monolayers with increasing surface pressure. Greater proximity of monomers at a higher surface pressure allows for a more effective radical propagation at a given time and, thus, it leads to longer polymer units.

Photopolymerization of BLMs prepared from **1** resulted in decreased trans-membrane resistances.[39] This was the consequence of reducing the average area occupied by each surfactant—a situation quite similar to that found for monolayers.

In sharp contrast to monolayers, the average degree of photopolymerization of surfactant vesicles, even at comparably low irradiation levels, was found to be much smaller (2–10).[20] Formation of much shorter polymers is the consequence of the absence of puckering and of much looser surfactant packing in vesicles as compared to monolayers. Molecular packing and organization is clearly an important parameter which influences polymerization-dependent organizational changes in the different membrane mimetic systems.

Acknowledgment. Support of this work by the National Science Foundation is gratefully acknowledged. We are also grateful to Professor Roger Leblanc for providing the facilities of his laboratories and to G. Munger and D. Ducharme for practical assistance. Ranieri Rolandi was partially supported by the Comitato Nazionale per le Scienze Fisiche of the CNR (contributo di ricerca N.87.00533.02).

Registry No. 1, 96478-22-7; **1** (homopolymer), 96478-23-8; **2**, 93253-93-1; **2** (homopolymer), 96478-21-6; **3**, 96499-12-6; **3** (homopolymer), 96499-13-7; **4**, 120853-59-0; **4** (homopolymer), 120853-60-3; **5**, 107-64-2.

Supplementary Material Available: An appendix outlining the derivation of the PPM and CPM approaches (9 pages). Ordering information is available on any current masthead page.

(39) Rolandi, R.; Flom, S. R.; Dillon, I.; Fendler, J. H. *Prog. Colloid Polym. Sci.* **1987**, *73*, 134–141.